

Immunogenicity evaluation of an Alum-adjuvanted recombinant prefusion RBD-Fd SARS-CoV-2 protein subunit produced in Glycoengineered *Pichia pastoris*

Andri Wardiana^{1*}, Hariyatun Hariyatun¹, Dian Fitria Agustiyanti¹, Yana Rubiyana¹, Alfi Taufik Fathurahman¹, Herjuno Ari Nugroho², Endah Puji Septisetyani¹, Popi Hadi Wisnuwardhani¹, Sugiyono Saputra², A'liyatur Rosyidah³, Syaiful Rizal⁴, Hastuti Handayani S. Purba¹, Kartika Sari Dewi¹, Nissa Arifa¹, Ratih Asmana Ningrum¹, Wien Kusharyoto¹

¹Research Centre for Genetic Engineering, National Research and Innovation Agency, KST Soekarno BRIN, Bogor, Indonesia.

²Research Centre for Applied Microbiology, National Research and Innovation Agency, KST Soekarno BRIN, Bogor, Indonesia.

³Research Centre for Vaccine and Drugs, National Research and Innovation Agency, KST Soekarno BRIN, Bogor, Indonesia.

⁴Research Centre for Applied Zoology, National Research and Innovation Agency, KST Soekarno BRIN, Bogor, Indonesia.

ARTICLE HISTORY

Received on: 15/07/2025

Accepted on: 17/09/2025

Available Online: XX

Key words:

RBD-Fd protein subunit,
Pichia pastoris Glycoswitch,
Aluminium hydroxide,
COVID-19, T cell activation.

ABSTRACT

The global coronavirus disease 2019 (COVID-19) pandemic, caused by severe acute respiratory syndrome coronavirus 2 (SARS-CoV-2), has accelerated vaccine development worldwide. While whole inactivated virus vaccines have reduced the incidence of severe disease and mortality, their effectiveness against emerging variants is limited. mRNA vaccines offer broader protection but face challenges in cost, production, and storage. Protein subunit vaccines targeting the viral spike (S) protein present a promising alternative due to their safety and scalability. In this study, we developed a recombinant protein subunit using the receptor-binding domain (RBD) of the SARS-CoV-2 spike protein, fused with a foldon domain (RBD-Fd) to promote trimer formation. The protein was expressed in *Pichia pastoris* GlycoSwitch® to achieve human-like glycosylation and was formulated with aluminium hydroxide (Alhydrogel®/Alum) to enhance immunogenicity. The resulting prototype protein subunit was evaluated in mice via subcutaneous injection at doses of 5 µg or 10 µg. Results showed that the alum-adjuvanted RBD-Fd formulation induced a strong antibody response following two doses at both concentrations. However, it generated only a partial T cell response with CD8⁺ T cell activation but no corresponding CD4⁺ response. These findings highlight the potential of prefusion RBD-based protein subunit and support further optimization to enhance cellular immunity.

1. INTRODUCTION

The world has been facing coronavirus disease 2019 (COVID-19) caused by severe acute respiratory syndrome coronavirus 2 (SARS-CoV-2) for more than 3 years [1]. This virus was first identified in the Wuhan area of China and subsequently spread to nearly all countries [2]. Researchers

worldwide are working to develop a vaccine against SARS-CoV-2 to prevent the spread of COVID-19. The first vaccine launched in an emergency and that has passed a clinical trial (phase III) is a whole, attenuated, or inactivated virus [3]. mRNA vaccines have demonstrated higher efficacy against various viral strains, but their production is costly, and they require complex cold-chain logistics to maintain stability [4–6]. Additionally, recent research has raised concerns about the long-term effects and biodistribution of mRNA vaccines, underscoring the need for global replication studies to confirm these findings and ensure their safety [7]. As an alternative, many researchers have developed protein subunit-based COVID-19 vaccines [8].

*Corresponding Author

Andri Wardiana, Research Centre for Genetic Engineering, National Research and Innovation Agency, KST Soekarno BRIN, Bogor, Indonesia
E-mail: andr027@brin.go.id

Protein subunit vaccines utilize specific proteins from the virus to stimulate the immune response in the body. The SARS-CoV-2 virus comprises several structural proteins, including spike, envelope, membrane, and nucleoprotein. The protein spike (S) is the most commonly used in the development of the COVID-19 vaccine due to its high antigenicity and immunogenicity [9]. The spike protein consists of two subunits, S1 and S2. The S1 subunit plays a crucial role in recognizing and binding to the host cell receptor, angiotensin-converting enzyme 2, through its receptor binding domain (RBD). In contrast, the S2 subunit mediates the fusion process between the viral membrane and the host cell [10].

In this study, we design a perfusion structure of RBD Spike SARS-CoV-2 as a prototype subunit protein, fused with the foldon domain (RBD-Fd) to form a trimeric structure. The protein was produced using the glycoengineered *Pichia pastoris* (*P. pastoris*) yeast GlycoSwitch[®], which allows for the controlled production of proteins with human-like glycosylation [11]. The use of *P. pastoris* engineered with human-like glycosylation overcomes the limitations of bacterial hosts, which lack glycosylation, and conventional yeast, which generate non-human glycan structures. This approach enhances the translational potential, yielding an active and immunologically compatible protein subunit vaccine candidate [12,13]. In addition, previous studies have shown the effectiveness of the prefusion conformation of the spike protein, resulting in protein stability that enhances the potency of neutralizing antibody responses [14–16].

In general, the effectiveness of vaccines relies not only on the antigen but also on adjuvants, which are frequently used to stimulate the immune system more effectively. The advantages of adjuvants include a reduction of the amount of antigen required for each vaccination dose and the number of vaccination sessions. Additionally, adjuvants also improve the stability of the antigen component by increasing its half-life; therefore, enhancing its immunogenicity [17,18]. In this study, aluminium hydroxide, Alhydrogel[®] (Alum), was used as an adjuvant to the antigen of RBD-Fd. Aluminium adjuvants have an excellent safety profile, are inexpensive, and work well with many of the different vaccine antigens in currently licensed vaccines [19].

Our research performed protein expression, purification, and characterization studies, followed by an investigation of biological efficacy using animal studies. We demonstrate that the formulation of alum-adjuvanted prefusion foldon fusion RBD spike of SARS-CoV-2 induces a robust antibody response, accompanied by a partial T cell response in mice.

2. MATERIALS AND METHODS

2.1. Protein production

The RBD-Fd protein was expressed using the *P. pastoris* GlycoSwitch[®] system, a genetically modified yeast strain (s10) with mannosidase knockdown to minimize high-mannose glycan structures (BioGrammatics, Inc., California, USA). Transformation was performed via electroporation using the Gene Pulser Xcell system (Bio-Rad, California, USA)

with a plasmid construct encoding a codon-optimized RBD-Fd gene comprising the Wuhan strain RBD fused to a foldon sequence via a GS flexible linker. The gene was inserted into the PD902 vector under control of the methanol-inducible AOX promoter (ATUM, California, USA) for efficient expression in yeast. Transformed cells were initially cultured in yeast peptone dextrose solid medium containing Zeocin (Gibco, New York, USA) for clone selection, followed by culture in Buffered Glycerol Complex Medium and induction of protein expression in Buffered Methanol-Complex Medium containing 1% methanol. The culture was incubated at 30°C and 200 rpm, with methanol induction every 24 hours. Cells were harvested on day 4, and the supernatant was collected for downstream processing.

2.2. Protein purification and formulation

The purification of the RBD-Spike protein was performed using an ÄKTA Avant system (Cytiva, Massachusetts, USA), following the manufacturer's protocols. The culture supernatant was first filtered through a 0.45 µm or 0.2 µm membrane filter (Corning, Arizona, USA) prior to a three-step purification process. This included protein capture using an ion-exchange column, followed by an intermediate purification step with hydrophobic interaction chromatography, and a final polishing step using size exclusion chromatography. In the initial stage, the filtered supernatant was applied to a pre-equilibrated HiTrap ANX FF (high sub) (Cytiva, Massachusetts, USA) column with binding buffer, containing 20 mM Tris-Cl, pH 9, at a flow rate of 0.5 ml/minute. The column was washed with binding buffer, followed by an elution step using a buffer containing 20 mM Tris-Cl, 1 M NaCl, pH 9. The eluate fractions were confirmed by SDS-PAGE and Slot Blot using anti-RBD primary antibodies. Samples containing the target protein were then supplemented with ammonium sulfate to a final concentration of 1 M, and the pH was adjusted to 7. The sample was then purified using the Hydrophobic Interaction Chromatography method with a HiScreen Phenyl FF (high sub) (Cytiva, Massachusetts, USA) column, which was pre-equilibrated with binding buffer containing 50 mM Na-phosphate and 1.7 M ammonium phosphate. This was followed by a washing step using the same buffer. Then, a buffer containing 50 mM Na-phosphate at pH 7 was applied to elute the protein target, and the positive fractions were collected for further purification steps. The final purification stage was performed through a Hi/Prep 16/60 Sephacryl S-200 HR column (Cytiva, Massachusetts, USA). Before purification, the sample was desalted with 1 × Phosphate Buffered Saline (PBS) and concentrated using an Amicon ultra centrifugal column with a 10 kDa molecular weight cutoff (Merck, Darmstadt, Germany). Up to 2 ml of sample was injected into the column, and the PBS 1 × was used to elute the sample with a flow rate of 0.5 ml/minute. All fractions that had peaks were checked using SDS-PAGE, Slot Blot, and Western Blot. The purification results were concentrated using a 10 kDa cutoff Amicon column (Merck, Darmstadt, Germany). Protein concentration was measured using the Pierce BCA Protein Assay Kit (Thermo Fisher Scientific, Massachusetts, USA). The purified protein

is then formulated with adjuvant Alum (Invivogen, California, USA) for biological tests.

2.3. Animals and animal ethics

This study used 30 specific pathogen-free (SPF) female BALB/c mice, aged 6–8 weeks, which were obtained from Nomura Siam International Co., Ltd, Thailand. The sample size was calculated using the Federer formula [20]. Mice were housed for 28 days in a closed-cage system within an ABSL-3 facility under controlled conditions, including a 12-hour light/dark cycle and *ad libitum* access to food and water throughout the experiment. All of the studies were approved by the Animal Care and Use Ethics Committee of the National Research and Innovation Agency (BRIN), No. 016/KE.02/SK/6/2022.

2.4. Immunization

Purified recombinant RBD protein at doses of 5 µg or 10 µg was mixed with 50 µg of aluminium hydroxide adjuvant and 1 × PBS, and administered subcutaneously in a total volume of 0.2 ml. Animals were divided into six groups ($n = 5$ per group): Group 1 received no treatment; Group 2 received PBS (placebo) on days 1 and 14; Group 3 received a single dose of 5 µg RBD on day 1; Group 4 received a single dose of 10 µg RBD on day 1; Group 5 received 5 µg RBD on days 1 and 14; and Group 6 received 10 µg RBD on days 1 and 14 (Table 1). On day 28, all mice were euthanized via intraperitoneal injection of overdosed pentobarbital. Blood was collected via intracardiac puncture during termination, and necropsy was performed to collect the spleen aseptically for further analysis.

2.5. Serum and spleen preparation

The blood samples from each group were centrifuged at 1,000–2,000 × g for 10–15 minutes in a refrigerated centrifuge to separate the serum from the blood clot. The serum samples were stored at –80°C for further Enzyme-linked immunosorbent assay (ELISA) analysis. On the other hand, the spleen was washed three times with PBS in a petri dish to remove non-specific debris and blood from the sample. The sample was mechanically disrupted by pressing the tissue with the base of a syringe to create a single-cell suspension, which was then filtered through Falcon® 70 µm Cell Strainers (Corning, Arizona, USA) to remove clumps and transferred to a polypropylene tube. PBS was added to bring the volume to 10 ml, and the suspension was centrifuged at 2,500 rpm for 5 minutes at 4°C. The resulting pellet was resuspended in 1 ml of PBS. After that, 200 µl of the cell suspension was transferred to

a microtube, mixed with 500 µl of PBS, and centrifuged again at 2,500 rpm for 5 minutes at 4°C. Cell numbers were aliquoted at 1×10^6 cells/well in 200 µl of PBS and kept on ice for flow cytometry analysis.

2.6. Flow cytometry

The cells were incubated with FITC-conjugated CD8a Monoclonal Antibody (Invitrogen, Thermo Fisher Scientific, Massachusetts, USA) and PE-conjugated anti-CD4 monoclonal antibody (Invitrogen, Thermo Fisher Scientific, Massachusetts, USA) for 30 minutes at 4°C in the dark. The cells were washed three times with PBS, resuspended in 200 µl PBS, and subsequently analyzed by flow cytometry to assess CD4⁺ and CD8⁺ T cell populations using Attune NxT Flow Cytometer (Thermo Fisher Scientific, Massachusetts, USA) in the FITC and PE channels at 498/517 nm and 565/576 nm for excitation/emission maximum, respectively.

2.7. ELISA for antibody response

An in-house ELISA was performed to investigate the presence of anti-RBD antibodies in the serum sample. Briefly, an ELISA plate (Nunc, Illinois, USA) was precoated with the antigen at approximately 50 ng/well in sodium carbonate buffer at pH 9.6. After blocking with 5% skim milk in PBS-T (PBS containing 0.05% (v/v) Tween-20) for about 2 hours, the plate was then washed three times with PBS-T. Then, a freshly prepared dilution of serum (1:100) of each treatment group was added to an RBD-coated plate and incubated overnight at 4°C. After washing with PBS-T, anti-mouse IgG conjugated with HRP (Thermo Fisher Scientific, Massachusetts, USA) was added and incubated for about 2 hours at room temperature. The signal from the antibody reaction was developed by adding ABTS (Sigma-Aldrich, St. Louis, USA) as an HRP substrate. After color development, the optical density of each well was determined using a microplate reader, Multiskan FC Microplate Photometer (Thermo Fisher Scientific, Massachusetts, USA), at 405 nm.

2.8. Statistical analysis

Statistical significance was determined using one-way analysis of variance (ANOVA) followed by Dunnett's multiple comparisons test to compare each treatment group with the untreated group. All analyses were performed using GraphPad Prism version 8. Data were presented as mean ± standard deviation (SD). A p -value < 0.01 was considered statistically significant.

3. RESULTS AND DISCUSSION

3.1. Expression of trimeric RBD-Fd

Figure 1A shows the structural design of the trimeric foldon-fused RBD of the SARS-CoV-2 spike protein for subunit antigen development. The foldon domain, derived from T4 fibrin, was employed to facilitate trimerization of the RBD, mimicking the native trimeric architecture of the viral spike protein. This design aims to enhance antigen presentation and potentially improve immunogenicity by better mimicking the natural viral structure [21].

Table 1. Group of treatment and recombinant RBD-Fd dose.

Group	Treatment	Number of mice
1	Control (Untreated)	5
2	Placebo (PBS only)	5
3	RBD-Fd dose 5 µg	5
4	RBD-Fd dose 10 µg	5
5	RBD-Fd dose 5 µg + booster	5
6	RBD-Fd dose 10 µg + booster	5

The recombinant RBD-Fd protein was expressed in a glycoengineered *P. pastoris* strain engineered to produce human-like glycosylation patterns. The target protein was secreted into the culture medium, and the sample used for analysis was collected from the supernatant. To verify the expression and oligomeric state of the construct, a Western blot was performed using an anti-RBD SARS-CoV-2 antibody (Fig. 1B). The protein sample was run on a reducing SDS-PAGE gel. Still, it was prepared with a non-reducing sample buffer and not boiled, allowing for partial preservation of non-covalent interactions. The blot revealed a prominent band at a higher

molecular weight, corresponding to the trimeric form of the RBD-Fd fusion protein. Additionally, a lower molecular weight band was observed at the expected size of approximately 31 kDa, indicating the monomeric form of the protein. This is likely due to partial dissociation of the trimer under the denaturing gel conditions. The presence of both trimeric and monomeric forms suggests that, although the foldon domain effectively promotes trimerization, some subunit dissociation occurs during electrophoresis. This phenomenon is common when analyzing multimeric proteins under denaturing conditions and does not necessarily imply structural instability under physiological conditions [22]. Further confirmation of the trimeric state in native conditions could be pursued using techniques such as size-exclusion chromatography coupled with multi-angle light scattering or blue native PAGE [23].

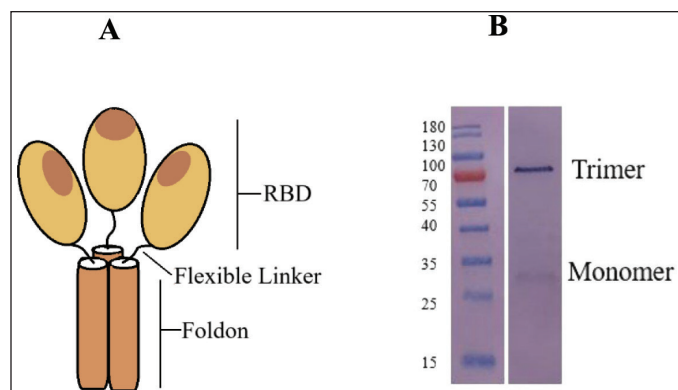


Figure 1. (A) The trimeric structure of the prefusion foldon-fused receptor-binding domain (RBD) of the SARS-CoV-2 spike protein was achieved by linking the foldon domain to the C-terminus of the RBD via a glycine-serine (GS) flexible linker, promoting trimerization of the protein in cells. (B) Western blot analysis using anti-RBD SARS-CoV-2 antibody showing trimeric and monomeric forms of RBD-Fd expressed in glycoengineered *P. pastoris*. Molecular weight marker: PageRuler Prestained Protein Ladder, 10–180 kDa (Thermo Fisher Scientific).

3.2 Protein purification

The purification workflow and subsequent analysis of the RBD-Fd protein expressed in culture supernatant using a multistep chromatography strategy are shown in Figure 2A. The workflow presents a stepwise purification scheme starting with ion exchange chromatography (IEX) using a weak anion exchange column, followed by hydrophobic interaction chromatography (HIC), and finalized with size exclusion chromatography (SEC) for polishing. This sequential approach was designed to ensure high purity and structural integrity of the recombinant RBD-Fd protein. IEX enabled effective initial capture of the target protein based on charge interactions, while HIC further removed hydrophobic contaminants. The final SEC step was critical for separating trimeric RBD-Fd from aggregated species or low-molecular-weight impurities.

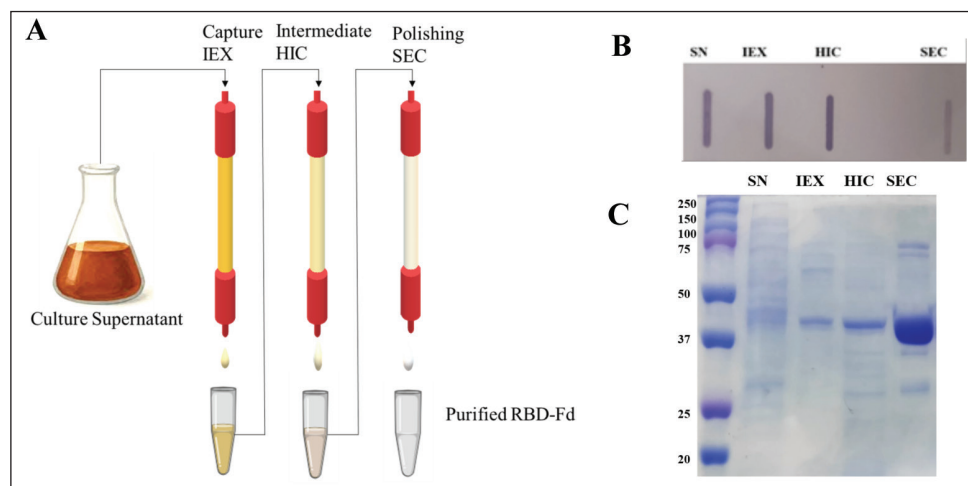


Figure 2. Purification of RBD-Fd from cell culture supernatant and analysis of eluates. (A) Schematic representation of the sequential chromatography purification strategy. The chromatography step starts with ion exchange chromatography (IEX) for capture, followed by hydrophobic interaction chromatography (HIC), and concluding with a polishing step using size exclusion chromatography (SEC). (B) Slot blot analysis using a monoclonal antibody specific to the receptor-binding domain (RBD) of the SARS-CoV-2 spike protein. (C) SDS-PAGE analysis was performed under reducing and denaturing conditions (boiled sample buffer). The SEC eluate was concentrated using a 10 kDa molecular weight cut-off Amicon Ultra centrifugal filter. Molecular weight marker: Precision Plus Protein™ Standards, 10–250 kDa (Bio-Rad).

To evaluate the presence, integrity, and purity of the recombinant RBD-Fd protein following multistep chromatography, slot blot and SDS-PAGE analyses were performed on the eluate of every single step of purification. Figure 2B shows the slot blot analysis, performed using an anti-RBD SARS-CoV-2 antibody, which demonstrated the presence of the target protein in the eluate fractions collected from each purification step. These results confirm that the RBD-Fd fusion protein was successfully retained and eluted during each chromatography stage, indicating efficient recovery throughout the process. To further evaluate protein purity, SDS-PAGE analysis was conducted on the same fractions (Fig. 2C). The SDS-PAGE results revealed a progressive improvement in purity after each purification step, with the final size exclusion chromatography yielding a dominant band corresponding to the expected molecular weight of the RBD-Fd fusion protein. Minor bands, possibly representing host cell proteins or degradation products, were substantially reduced after the final polishing step, indicating the effective removal of impurities. These results demonstrate the effectiveness of the multistep chromatography approach in purifying the RBD-Fd protein to high homogeneity, a critical prerequisite for downstream biochemical or immunological characterization.

3.3. Immunogenicity study

Figure 3 illustrates the schematic of the *in vivo* study design used to evaluate the immunogenicity of the purified RBD-Fd protein. Female SPF BALB/c mice were assigned to different treatment groups, including untreated, PBS-only, and formulation-treated groups (5 μ g and 10 μ g doses). Every treated group received a single dose of the formulation or PBS on Day 1. To assess the effect of a booster immunization, two formulation-treated groups received an additional dose on Day 14. The study was terminated on Day 28, at which point blood and spleen samples were collected for subsequent immunological analysis. This study design allowed for the

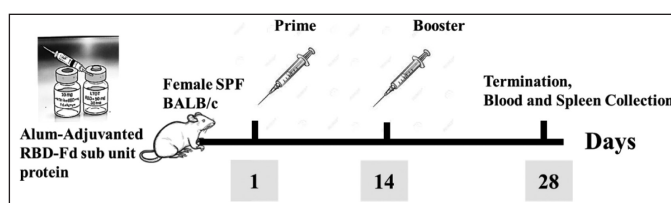


Figure 3. Schematic of the *in vivo* study design. Female SPF BALB/c mice received the assigned dose on Day 1 across all groups. A booster dose was administered on Day 14 to the designated group. The study concluded on Day 28, followed by blood and spleen collection.

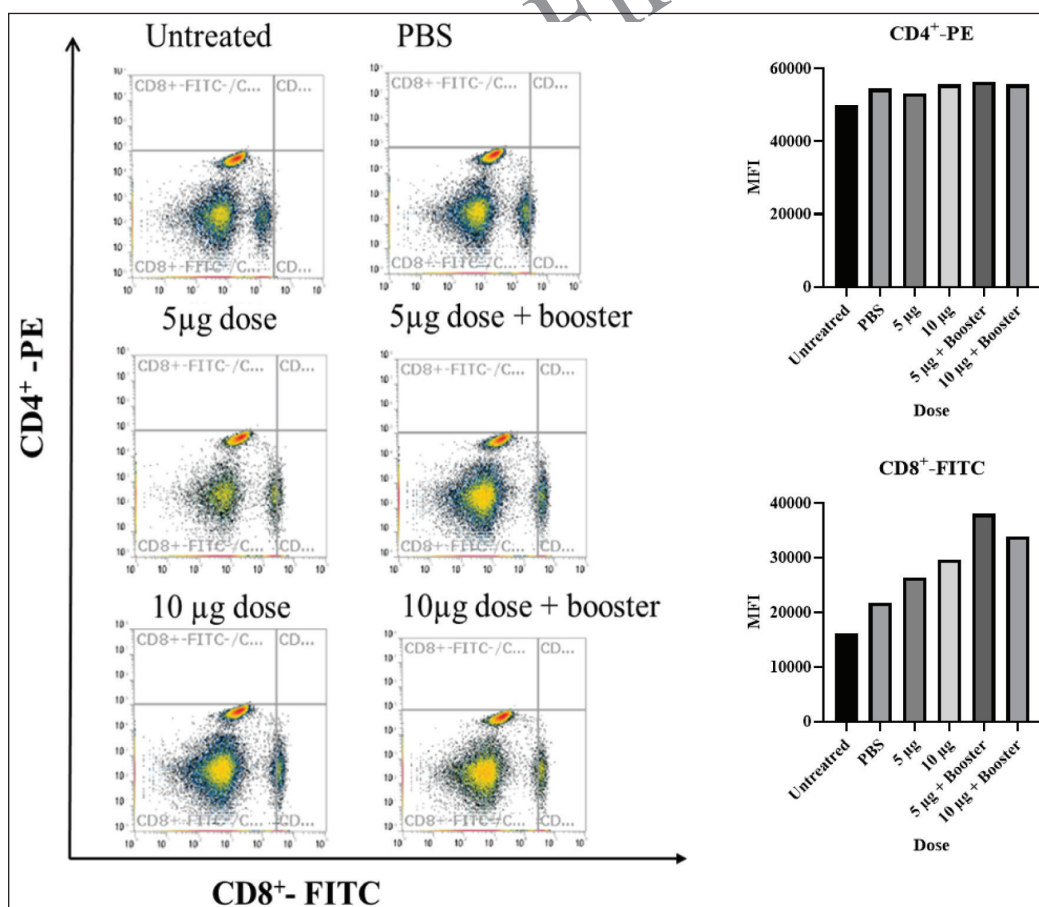


Figure 4. Flow cytometric analysis of splenocytes after immunization, showing CD4⁺ (PE) and CD8⁺ (FITC) T cell responses. The bar chart represents the mean fluorescence intensity (MFI) for each channel.

assessment of both primary and secondary immune responses. The inclusion of a booster group enables comparison of immune kinetics and magnitude between single-dose and two-dose regimens. The 14-day interval between prime and boost is commonly used in murine models and was selected to mimic accelerated immunization schedules suitable for pandemic response scenarios. Termination on Day 28 provided sufficient time for the development of measurable humoral and potential cellular immune responses, while minimizing the risk of age-related variability in immune function [24].

Flow cytometric analysis of splenocytes harvested following immunization was conducted to evaluate the T cell response through CD4⁺ and CD8⁺ markers (Fig. 4). The data demonstrate a partial immune response exclusively in CD8⁺ T cells, with no detectable response in CD4⁺ T cells across all tested groups. In the CD8⁺ T cell population, both the 5 μ g and 10 μ g single-dose groups showed increased mean fluorescence intensity (MFI) signals compared to controls. Booster immunization further enhanced the response relative to single-dose groups. However, the response was not dose-dependent, as the 10 μ g booster group exhibited a lower MFI signal than the 5 μ g booster group. These findings suggest that booster administration, rather than antigen dose within the 5–10 μ g range, was the key factor enhancing CD8⁺ T cell response. In contrast, untreated and PBS-only groups showed no activation of either CD4⁺ or CD8⁺ T cells, confirming the specificity of the formulation-induced immune response. These findings suggest that the formulation predominantly activates CD8⁺ cytotoxic T lymphocytes, with minimal or no engagement of CD4⁺ helper T cells. The lack of a CD4⁺ response may reflect the nature of the antigen processing pathway [25] or the adjuvant profile [26], which favors cross-presentation and MHC class I-restricted CD8⁺ activation [27]. Overall, while CD8⁺ T cell responses are promising, the lack of CD4⁺ T cell activation may have implications for long-term memory and humoral support. CD4⁺ T cells play a vital role in helping CD8⁺ T cells mature into memory cells and in guiding B cells to produce effective antibodies [28–31]. Therefore, further investigation into the formulation or optimization of adjuvants is needed to achieve a more balanced immune profile.

The ELISA results in Figure 5 demonstrate that a significant antibody response against the SARS-CoV-2 RBD protein was observed only in the booster immunization groups at both 5 μ g and 10 μ g doses. In contrast, single-dose immunization at either dose, as well as the PBS control group, failed to elicit a detectable antibody response, with signal levels comparable to the untreated control. Importantly, both booster groups showed comparable antibody titers, suggesting that increasing the antigen dose from 5 μ g to 10 μ g did not further enhance the immune response. These findings are consistent with a previous study, which reported that a vaccine candidate based on an RBD trimer protein subunit induced a robust humoral response only after two doses [32]. Moreover, recent preclinical evaluations of an RBD-trimeric subunit vaccine demonstrated that a 25 μ g dose was sufficient to elicit antibody production, while booster immunizations clearly improved the seroconversion rate [33]. Taken together, these observations suggest that a single dose of 5–10 μ g may be insufficient to

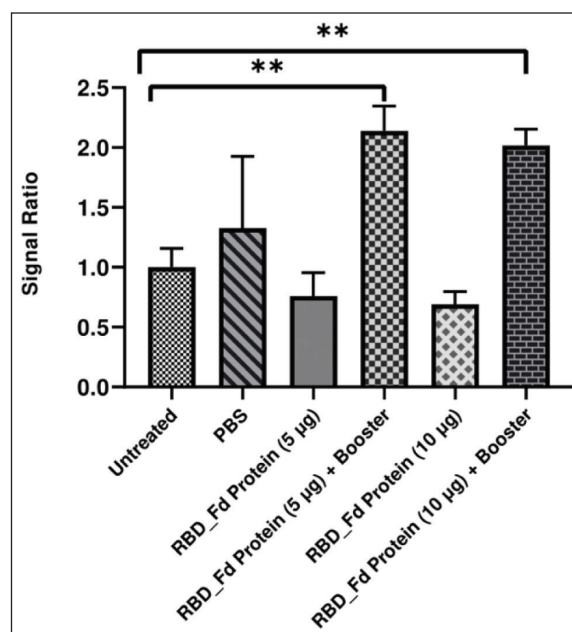


Figure 5. ELISA analysis of serum samples against the SARS-CoV-2 RBD protein. The data represent the signal ratio of the treated groups relative to the untreated control group, measured at an optical density (OD) of 405 nm. Data are represented as the mean \pm SD. One-way ANOVA analyzed data with Dunnett's multiple comparisons test. $**p < 0.01$.

trigger a measurable immune response, thereby underscoring the importance of booster immunization for achieving robust humoral immunity. Statistical analysis using one-way ANOVA confirmed that the antibody responses in both booster groups were significantly higher than those in the untreated group ($p < 0.01$), emphasizing the critical role of booster immunization in eliciting a robust humoral response [34,35].

Overall, these results confirm the successful expression, secretion, initial structural characterization, purification, and immunogenicity studies of the trimeric RBD-Fd fusion protein in glycoengineered yeast *P. pastoris*, supporting its potential as a viable subunit protein as a vaccine candidate against SARS-CoV-2. Building on previous studies, yeast-expressed subunit vaccines represent a highly advantageous platform, offering a unique combination of safety, scalability, and strong immunogenicity. These attributes not only reinforce the translational relevance of our findings but also highlight their potential for advancement into real-world vaccine development. Moreover, the demonstrated capacity of yeast-based systems to induce robust immune responses through simplified production further supports their suitability for rapid and cost-effective clinical translation [36,37].

4. CONCLUSION

This study successfully demonstrated the expression, purification, and immunogenicity of a trimeric SARS-CoV-2 RBD-Fd fusion protein produced in glycoengineered *P. pastoris*. The fusion of the foldon domain to the RBD effectively promoted trimerization, as shown by Western blot analysis, mimicking the native structure of the viral spike protein. The

multistep purification strategy comprising IEX, HIC, and SEC yielded a highly purified antigen suitable for *in vivo* studies.

Immunogenicity evaluation in SPF BALB/c mice model revealed that booster immunization was essential for eliciting both humoral and cellular immune responses. ELISA analysis confirmed that significant antibody responses were observed only in animals receiving a booster dose, with no additional benefit observed at the higher (10 µg) dose compared to the lower (5 µg) dose. Flow cytometry results showed a selective induction of CD8⁺ T cell responses, particularly in the booster groups, while CD4⁺ T cell activation remained undetectable. The absence of an immune response in both untreated and PBS-only controls confirmed the specificity of the immune activation.

These results provide proof-of-concept for yeast-expressed trimeric RBD-Fd as a scalable recombinant protein subunit platform. However, further optimization is required to achieve balanced humoral and cellular immunity. Future work will focus on neutralization assays to validate the functional activity of the elicited antibodies, adjuvant screening to enhance immunogenicity, and viral challenge studies to assess protective efficacy. Expanding the evaluation to include different mouse strains, both sexes, and non-human primate models will be critical for improving the predictive value of preclinical data and bridging the gap toward clinical testing.

5. ACKNOWLEDGMENT

This study was supported by funding from the Consortium of Research and Innovation COVID-19 LPDP-Ministry of Research and Technology/National Research and Innovation Agency (Kemenristek/BRIN) (No Kep 67/LPDP/2020) and the DIPA Program of Research Organization for Life Sciences and Environment BRIN (No 9/HI/HK/2022). The authors thank Mr. Dadang Supritana for his technical assistance in the animal facility during the *in vivo* experiments.

6. AUTHOR CONTRIBUTIONS

All authors made substantial contributions to conception and design, acquisition of data, or analysis and interpretation of data; took part in drafting the article or revising it critically for important intellectual content; agreed to submit to the current journal; gave final approval of the version to be published; and agree to be accountable for all aspects of the work. All the authors are eligible to be an author as per the International Committee of Medical Journal Editors (ICMJE) requirements/guidelines.

7. CONFLICTS OF INTEREST

The authors report no financial or any other conflicts of interest in this work.

8. ETHICAL APPROVALS

Ethical approvals details are given in the 'MATERIALS and METHODS' section.

9. DATA AVAILABILITY

All data generated and analyzed are included in this research article.

10. PUBLISHER'S NOTE

All claims expressed in this article are solely those of the authors and do not necessarily represent those of the publisher, the editors and the reviewers. This journal remains neutral with regard to jurisdictional claims in published institutional affiliation.

11. USE OF ARTIFICIAL INTELLIGENCE (AI)-ASSISTED TECHNOLOGY

The authors declare that they have not used artificial intelligence (AI)-tools for writing and editing of the manuscript, and no images were manipulated using AI.

REFERENCES

1. Naimi A, Yashmi I, Jebileh R, Imani Mofrad M, Azimian Abhar S, Jannesar Y, *et al.* Comorbidities and mortality rate in COVID-19 patients with hematological malignancies: a systematic review and meta-analysis. *J Clin Lab Anal.* 2022;36(5):e24387. doi: <https://doi.org/10.1002/jcla.24387>
2. Koupaei M, Naimi A, Moafi N, Mohammadi P, Tabatabaei FS, Ghazizadeh S, *et al.* Clinical characteristics, diagnosis, treatment, and mortality rate of TB/COVID-19 coinfecting patients: a systematic review. *Front Med.* 2021;8:740593. doi: <https://doi.org/10.3389/fmed.2021.740593>
3. Hotez PJ, Bottazzi ME. Whole inactivated virus and protein-based COVID-19 vaccines. *Annu Rev Med.* 2022;73:55–64. doi: <https://doi.org/10.1146/annurev-med-042420-113212>
4. Kowalzik F, Schreiner D, Jensen C, Teschner D, Gehring S, Zepp F. mRNA-based vaccines. *Vaccines.* 2021;9(4):390. doi: <https://doi.org/10.3390/vaccines9040390>
5. Gote V, Bolla PK, Kommineni N, Butreddy A, Nukala PK, Palakurthi SS, *et al.* A comprehensive review of mRNA vaccines. *Int J Mol Sci.* 2023;24(3):2700. doi: <https://doi.org/10.3390/ijms24032700>
6. Leong KY, Tham SK, Poh CL. Revolutionizing immunization: a comprehensive review of mRNA vaccine technology and applications. *Viol J.* 2025;22(1):71. doi: <https://doi.org/10.1186/s12985-025-02645-6>
7. Ota N, Itani M, Aoki T, Sakurai A, Fujisawa T, Okada Y, *et al.* Expression of SARS-CoV-2 spike protein in cerebral arteries: implications for hemorrhagic stroke Post-mRNA vaccination. *J Clin Neurosci.* 2025;136:111223. doi: <https://doi.org/10.1016/j.jocn.2025.111223>
8. Heidary M, Kaviar VH, Shirani M, Ghanavati R, Motahar M, Sholeh M, *et al.* A comprehensive review of the protein subunit vaccines against COVID-19. *Front Microbiol.* 2022;13:927306. doi: <https://doi.org/10.3389/fmicb.2022.927306>
9. Martínez-Flores D, Zepeda-Cervantes J, Cruz-Reséndiz A, Aguirre-Sampieri S, Sampieri A, Vaca L. SARS-CoV-2 vaccines based on the spike glycoprotein and implications of new viral variants. *Front Immunol.* 2021;12:701501. doi: <https://doi.org/10.3389/fimmu.2021.701501>
10. Huang B, Dai L, Wang H, Hu Z, Yang X, Tan W, *et al.* Serum sample neutralisation of BBIBP-CorV and ZF2001 vaccines to SARS-CoV-2 501Y.V2. *Lancet Microbe.* 2021;2(7):285. doi: [https://doi.org/10.1016/S2666-5247\(21\)00082-3](https://doi.org/10.1016/S2666-5247(21)00082-3)
11. Li H, Sethuraman N, Stadheim TA, Zha D, Prinz B, Ballew N, *et al.* Optimization of humanized IgGs in glycoengineered *Pichia pastoris*. *Nat Biotechnol.* 2006;24(2):210–5. doi: <https://doi.org/10.1038/nbt1178>
12. Choi BK, Actor JK, Rios S, D'Anjou M, Stadheim TA, Warburton S, *et al.* Recombinant human lactoferrin expressed in glycoengineered *Pichia pastoris*: effect of terminal N-acetylneuraminic acid on *in vitro* secondary humoral immune response. *Glycoconj J.* 2008;25(6):581–93. doi: <https://doi.org/10.1007/s10719-008-9123-y>

13. Liu B, Yin Y, Liu Y, Wang T, Sun P, Ou Y, *et al.* A vaccine based on the receptor-binding domain of the spike protein expressed in glycoengineered *pichia pastoris* targeting SARS-CoV-2 stimulates neutralizing and protective antibody responses. *Eng (Beijing)*. 2022;13:107–15. doi: <https://doi.org/10.1016/j.eng.2021.06.012>
14. Pallesen J, Wang N, Corbett KS, Wrapp D, Kirchdoerfer RN, Turner HL, *et al.* Immunogenicity and structures of a rationally designed prefusion MERS-CoV spike antigen. *Proc Natl Acad Sci U S A*. 2017;114(35):E7348–57. doi: <https://doi.org/10.1073/pnas.1707304114>
15. Hsieh CL, Goldsmith JA, Schaub JM, DiVenere AM, Kuo HC, Javanmardi K, *et al.* Structure-based design of prefusion-stabilized SARS-CoV-2 spikes. *Science*. 2020;369(6510):1501–5. doi: <https://doi.org/10.1126/science.abd0826>
16. Watterson D, Wijesundara DK, Modhiran N, Mordant FL, Li Z, Avumegah MS, *et al.* Preclinical development of a molecular clamp-stabilised subunit vaccine for severe acute respiratory syndrome coronavirus 2. *Clin Transl Immunol*. 2021;10(4):1269. doi: <https://doi.org/10.1002/cti2.1269>
17. Zhao T, Cai Y, Jiang Y, He X, Wei Y, Yu Y, *et al.* Vaccine adjuvants: mechanisms and platforms. *Signal Transduct Target Ther*. 2023;8(1):283. doi: <https://doi.org/10.1038/s41392-023-01557-7>
18. Facciola A, Visalli G, Laganà A, Di Pietro A. An overview of vaccine adjuvants: current evidence and future perspectives. *Vaccines*. 2022;10(5):819. doi: <https://doi.org/10.3390/vaccines10050819>
19. HogenEsch H, O'Hagan DT, Fox CB. Optimizing the utilization of aluminum adjuvants in vaccines: you might just get what you want. *Vaccines*. 2018;3(1):51. doi: <https://doi.org/10.1038/s41541-018-0089-x>
20. Rukmana A, Supardi LA, Sjatha F, Nurfadilah M. Responses of humoral and cellular immune mediators in BALB/c Mice to LipX (PE11) as seed tuberculosis vaccine candidates. *Genes (Basel)*. 2022;13(11):1954. doi: <https://doi.org/10.3390/genes13111954>
21. Tai W, Zhao G, Sun S, Guo Y, Wang Y, Tao X, *et al.* A recombinant receptor-binding domain of MERS-CoV in trimeric form protects human dipeptidyl peptidase 4 (hDPP4) transgenic mice from MERS-CoV infection. *Virology*. 2016;499:375–82. doi: <https://doi.org/10.1016/j.virol.2016.10.005>
22. Papanikolopoulou K, Forge V, Goeltz P, Mittraki A. Formation of highly stable chimeric trimers by fusion of an adenovirus fiber shaft fragment with the foldon domain of bacteriophage T4 fibritin. *J Biol Chem*. 2004;279(10):8991–8. doi: <https://doi.org/10.1074/jbc.M311791200>
23. Knetsch TGJ, Ubbink M. Production and compositional analysis of full-length influenza virus hemagglutinin in Nanodiscs: insights from multi-angle light scattering. *Protein Expr Purif*. 2025;227:106641. doi: <https://doi.org/10.1016/j.pep.2024.106641>
24. Yang MC, Wang CC, Tang WC, Chen KM, Chen CY, Lin HH, *et al.* Immunogenicity of a spike protein subunit-based COVID-19 vaccine with broad protection against various SARS-CoV-2 variants in animal studies. *PLoS One*. 2023;18(3):283473. doi: <https://doi.org/10.1371/journal.pone.0283473>
25. Mettu RR, Charles T, Landry SJ. CD4+ T-cell epitope prediction using antigen processing constraints. *J Immunol Methods*. 2016;432:72–81. doi: <https://doi.org/10.1016/j.jim.2016.02.013>
26. Rapaka RR. How do adjuvants enhance immune responses? *eLife*. 2024;13:e101259. doi: <https://doi.org/10.7554/eLife.101259>
27. Rood JE, Yoon SK, Heard MK, Carro SD, Hedgepeth EJ, O'Mara ME, *et al.* Endogenous antigen processing promotes mRNA vaccine CD4+ T cell responses. *bioRxiv*. 2025; doi: <https://doi.org/10.1101/2025.03.11.642674>
28. Laidlaw BJ, Craft JE, Kaech SM. The multifaceted role of CD4(+) T cells in CD8(+) T cell memory. *Nat Rev Immunol*. 2016;16(2):102–11. doi: <https://doi.org/10.1038/nri.2015.10>
29. Painter MM, Mathew D, Goel RR, Apostolidis SA, Pattekar A, Kuthuru O, *et al.* Rapid induction of antigen-specific CD4(+) T cells is associated with coordinated humoral and cellular immunity to SARS-CoV-2 mRNA vaccination. *Immunity*. 2021;54(9):2133–42. doi: <https://doi.org/10.1016/j.immuni.2021.08.001>
30. Topchyan P, Lin S, Cui W. The role of CD4 T cell help in CD8 T cell differentiation and function during chronic infection and cancer. *Immune Netw*. 2023;23(5):41. doi: <https://doi.org/10.4110/in.2023.23.e41>
31. Xie L, Fang J, Yu J, Zhang W, He Z, Ye L, *et al.* The role of CD4(+) T cells in tumor and chronic viral immune responses. *MedComm*. 2023;4(5):390. doi: <https://doi.org/10.1002/mco2.390>
32. Su R, Shi Z, Li E, Zhu M, Li D, Liu X, *et al.* A Trim-RBD-GEM vaccine candidate protects mice from SARS-CoV-2. *Virology*. 2023;585:145–54. doi: <https://doi.org/10.1016/j.virol.2023.06.005>
33. Flórez L, Echeverri-De la Hoz D, Calderón A, Serrano-Coll H, Martínez C, Guzmán C, *et al.* Preclinical evaluation of the RBD-Trimeric vaccine: a novel approach to strengthening biotechnological sovereignty in developing countries against SARS-CoV-2 variants. *Travel Med Infect Dis*. 2025;64:102820. doi: <https://doi.org/10.1016/j.tmaid.2025.102820>
34. Kim E, Khan MS, Ferrari A, Huang S, Sammartino JC, Percivalle E, *et al.* SARS-CoV-2 S1 subunit booster vaccination elicits robust humoral immune responses in aged mice. *Microbiol Spectr*. 2023;11(3):436322. doi: <https://doi.org/10.1128/spectrum.04363-22>
35. Korosec CS, Dick DW, Moyles IR, Watmough J. SARS-CoV-2 booster vaccine dose significantly extends humoral immune response half-life beyond the primary series. *Sci Rep*. 2024;14(1):8426. doi: <https://doi.org/10.1038/s41598-024-58811-3>
36. Gebauer M, Hürliemann HC, Behrens M, Wolff T, Behrens SE. Subunit vaccines based on recombinant yeast protect against influenza A virus in a one-shot vaccination scheme. *Vaccine*. 2019;37(37):5578–87. doi: <https://doi.org/10.1016/j.vaccine.2019.07.094>
37. Lang Q, Huang N, Li L, Liu K, Chen H, Liu X, *et al.* Novel and efficient yeast-based strategies for subunit vaccine delivery against COVID-19. *Int J Biol Macromol*. 2025;294:139254. doi: <https://doi.org/10.1016/j.ijbiomac.2024.139254>

How to cite this article:

Wardiana A, Hariyatun H, Agustiyanti DF, Rubiyana Y, Fathurahman AT, Nugroho HA, Septisetyani EP, Wisnuwardhani PH, Saputra S, Rosyidah A, Rizal S, Purba HHS, Dewi KS, Arifa N, Ningrum RA, Kusharyoto W. Immunogenicity evaluation of an Alum-adjuvanted recombinant prefusion RBD-Fd SARS-CoV-2 protein subunit produced in Glycoengineered *Pichia pastoris*. *J Appl Pharm Sci*. 2025. Article in Press. <http://doi.org/10.7324/JAPS.2026.270912>